Influence of heat-treatment temperature on structural and electrical properties for $BaSrTiO_3$ compounds

H. A. Gatea[a,*], S. J. Shoja[b] , H. J. Albazoni[c]
[a]*Department Of Medical Physics, Al-Mustaqbal University College 51001, Hillah, Babylon, Iraq*
[b]*College Of Health& Medical Technology, Al-Ayen University, Iraq*
[c]*Collage Of Pharmacy, National University of Science and Technology, Dhi Qar, Iraq*

The sol-gel process was utilized in the production of the ferroelectric material $Ba_{0.7}Sr_{0.3}TiO_3$. Barium and strontium acetate were employed as sources for Ba and Sr, respectively, and Ti(IV) isopropoxide was used as a source for Ti. The acetic acid was utilized as a solvent for Ba and Sr acetate, whereas 2-methoxy ethanol was used as a stabilizer for Ti (IV) isopropoxide. The effect of high temperatures on electrical and structural were studied. The FESEM revealed the particle size of all samples with different temperatures. The XRD shows the $Ba_{0.7}Sr_{0.3}TiO_3$ samples have a tetragonal phase for all temperatures (1000, 1100, 1200˚C). The high temperatures impacted tetragonality and the lattice constant (a, c); the lattice constant decreased at higher temperatures. The ferroelectric sample sintered at 1000 degrees Celsius had dielectric characteristics that were inferior to those of the $Ba_{0.7}Sr_{0.3}TiO_3$sample sintered at 1100 and 1200ºC degrees Celsius. When the dielectric constant was graphed as a function of temperature, the Curie temperature appeared to be between (28-32) degrees Celsius.

(Received April 28, 2023; Accepted July 17, 2023)

Keywords: Ferroic materials Curie temperature, Ferroelectric materials, $BaSrTiO_3$

1. Introduction

Ferroelectrics are materials that exhibit spontaneous polarisation over a certain temperature range. They are a special type of pyroelectrics belonging to piezoelectric[1]. All these classes are formed of dielectric materials. Ferroelectric materials are dielectric materials with spontaneous polarization that can be reversed by an external electric field and retain polarization when removed[2][3][4]. Due to its high dielectric constant, low dissipation factor, adjustable dielectric constant at different frequencies, and low leakage current, barium strontium, titanate is a ferroelectric material now receiving much attention[5][6].

In perovskite structure (ABO3), A, B atoms have different valance electrons but different sizes or radii of atoms[7]. More features can be seen in the perovskite structure with Barium Strontium Titanate (BST) compounds, such as substituting one atom (A) from (B) or vice versa[8][6].

Barium Strontium Titanate (BST) belongs to the (ABO3) perovskite family of crystal structures (ABX3)[9]. It possesses crystalline properties similar to general perovskites with a cubic nature and with the chemical formula $Ba_{1-x}Sr_xTiO_3$[10]. The ferroelectric materials mentioned above, the solid solution composition of ferroelectric barium titanate ($BaTiO_3$) and paraelectric SrTiO3, BaSrTiO3 (BST) possess the best dielectric constant and have a relatively low loss over a wide range of frequencies, besides a low leakage current and large electric field tenability[11][12].

Barium Strontium Titanate (BST) compounds have emerged as very attractive materials over the last ten years[13]. BST compounds are increasingly used in new and important applications such as piezoelectric sensors, dynamic random dielectric access memory (DRAM),

* Corresponding author: hamed66gatea@gmail.com
https://doi.org/10.15251/JOR.2023.194.379

microwave phase shifter voltage-controlled oscillators, infrared detectors, frequency limiters, transformers, micro-electrical mechanical switches, resonators, pulse shaping, and sharping applications, and tunable Lange-couplers [14][15].

Perovskite materials can be prepared via a variety of methods, including mechanical methods (traditional mixed oxide processing) and chemical methods (flux growth of single crystals, chemical vapor deposition, co-precipitation, sol-gel). It can also be produced via the processing of metal alkoxides and the hydrothermal growth of fine powders [16][17][18].

The sol-gel method allows the mixing of metal oxides where mixing two or more phases can be controlled on both nanometer and molecular scales. Such systems comprise metal oxide composites desirable for various transition and main group metals[19][20]. BST compounds have a high dielectric constant and a low dissipation factor, which is why they are used in various capacitors. Several parameters of the sol-gel method affect the manufacture of material oxides[21]. Previous studies have shown that high temperature influences the electric properties, the microstructure, and the Curie temperature of $BaTiO_3$-based ceramics[22][23].

However, there is not enough information regarding the effects of high temperature on the dielectric and ferroelectric properties of $Ba_{0.7}Sr_{0.3}TiO_3$. Therefore, in this paper, $Ba_{0.7}Sr_{0.3}TiO_3$ was prepared via the conventional sol-gel method. This work's novelty stems from how crystal and particle sizes affect the dielectric constant values and the loss factor. The high heat treatment is the main reason why the size and shape of the crystals change.

The effects of high heat treatment on the microstructure and the dielectric and ferroelectric properties of $Ba_{0.7}Sr_{0.3}TiO_3$were then investigated in detail.

2. Experimental details

Ferroelectric $Ba_{0.7}Sr_{0.3}TiO_3$was prepared via sol-gel. The starting raw materials were high-purity Barium acetate (BDH Chemicals England, 99.95%), Strontium acetate (Sigma Aldrich, 99.9%), and Ti (IV) isopropoxide (97% Sigma Aldrich) as the sources of barium, strontium, and titanate, respectively. Acetic acid (Merck 99.8%) was used as the solvent, and 2-methoxy ethanol was used as a stabilizer for Ti (IV) isopropoxide.

To obtain stoichiometric proportions, an appropriate weight of barium acetate (0.08 mol) and strontium acetate (0.034 mol) powder were dissolved in a suitable volume of acetic acid (10 ml and 5 ml), respectively. Each solution was separately stirred for 60 min at 60˚C and then mixed to make up the (Ba, Sr) solution. This solution was refluxed in a reflux system (hotmintal (110 V), three-necked flask, reflux condenser), and the temperature of the solution at 110 °C was adjusted.

$$Sr(CH_3COO)_2 \;=\; SrCO_3$$

$$\mathrm{Ba}(CH_3COO)_2 = BaCO_3$$

$$(C_3H_7\ O)_4\,Ti = TiO_2$$

$$xBaCO_3 + (1-x)SrCO_3 + \ TiO_2 = Ba_x\,Sr_{1-x}TiO_3 + CO_2$$

The solution was refluxed at 110˚C for two hours (until the transparent solution turned slightly yellow). Then, 2-methoxy ethanol (2–4 ml) was added as the stabilizer to maintain the crystalline structure of Ti-isopropoxide at room temperature. The (Ba,Sr) solution was filled in a burette and added slowly (drop by drop) in the second solution (Ti(IV)). The final solution was then adjusted to a pH range of pH 3.5 to pH 5.

The solution was refluxed again in the reflux system until the solution turned into a white gel. Deionizing water was used to dilute the solution gel, and then a hot plate stirrer was used to stir the solution at 60˚C for one hour (1 h). The final solution was dried at 200˚C for 2 hours to separate the water completely and then again at 700˚C. The powders were calcined for a limited period (2 hours).

A mortar and pestle were used to obtain a fine powder. The BST nano-powder and fine powder were compacted in a cylindrical steel model with a (120 mm) internal diameter. In order to eliminate voids and porosity between the particles and size loss by compressing the particles closely together, the powder was compressed into a pellet shape. The final average dimension was (120 mm) in diameter, a thickness of (2.5–3.0 mm), and a pressure below (250–300 MPa).All samples were treated at three different temperatures (1000˚C, 1100˚C, and 1200˚C) using a programmable muffle furnace in an ambient atmosphere. A heat treatment cycle was developed to allow better densification and to avoid cracking at a heating rate of 5 °C/min. The pellets were cooled to room temperature at 8 °C.

The ferroelectric samples were examined via XRD (Bruker, Germany) with Cu Kα (40 kV and 30 mA). The ferroelectric sample's grain size and particle size were examined via Field emission Scanning Electron Microscope (FESEM, S-4700, Hitachi), and the electric properties were measured using an impedance analyzer, LCR".

3. Results and discussion

The XRD pattern of the $Ba_{0.7}Sr_{0.3}TiO_3$phase showed polycrystalline peaks related to the tetragonal perovskite phase along the (100), (101), (111), (200), (201), (211), (202), (221), (301) planes. The peak positions matched well with the PDF card no. (00-044-0093), this phase exhibited the P4 mm space group with (a =b 3.9771 Å and c = 3.9883 Å). Fig. 1 shows the polycrystalline structure of ferroelectric $Ba_{0.7}Sr_{0.3}TiO_3$ and the X-ray diffraction patterns at different temperatures.

It can be observed that ferroelectric $Ba_{0.7}Sr_{0.3}TiO_3$ sintered at 1200 °C had a BST phase with a perovskite structure, and there was no evidence of any additional phase, implying that Sr2+ ions have a unit cell that maintained the perovskite structure of the solid solution.

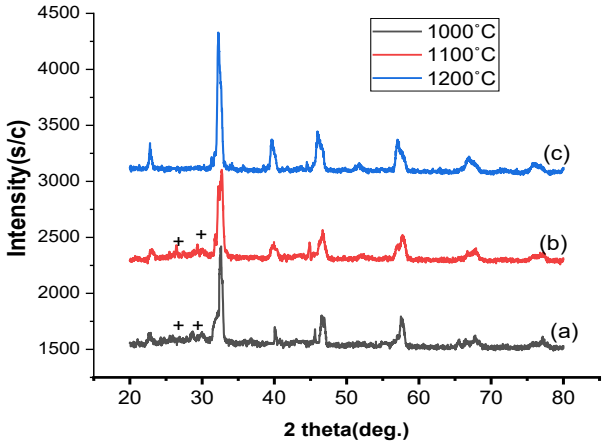

Fig. 1. XRD patterns of Ba0.7Sr0.3TiO3 ceramics sintered at different temperatures (1000, 1100, 1200˚C).

Ferroelectric Ba0.7Sr0.3TiO3 treating at 1000 °C and 1100 °C showed two weak diffraction peaks as a secondary phase (+, +) besides the peaks of the BST phase, which appeared at (2θ = 24.21°, 26.8°) and (28.8°) belonging to the intermediate oxycarbonates such as $Ba_2Ti_2O_5CO_3$, and (Ba,Sr) $Ti_2O_5CO_3$. The major peaks shifted toward higher 2θ angles when the Sr+ ions increased because of a decrease in the interatomic spacing of BST, affected by the radius of the Sr+ ion (1.13A°), which is smaller than the Ba+ ions (1.35 A°). All these results are shown in Table (1), which clearly shows that the standard and experimental d-space values depend on the angle and lattice constant.

Table 1. Structural parameters viz. angle values, Miller indices, inter-planar spacing for the phase of $Ba_{0.7}Sr_{0.3}TiO_3$ powders.

2Θ (degree) at 1000 °C	2Θ (degree)at 1100 °C	2Θ (degree) at 1200 °C	d-standard (Å)	$d_{Exp.}$ (Å) at 1000 °C	$d_{Exp.}$ (Å) at 1100 °C	$d_{Exp.}$ (Å) at 1200 °C	hkl
22.3363	22.6523	22.9745	3.96600	3.9611	3.8686	3.8547	(100)
31.7481	32.4398	32.724	2.80600	2.7931	2.7577	2.7344	(101)
39.1642	39.7661	39.9482	2.29000	2.2940	2.26401	2.2971	(111)
45.5621	46.218	46.4429	1.982300	1.9852	1.9526	1.9506	(200)
51.3012	51.8438	52.224	1.773500	1.7685	1.7621	1.7501	(201)
56.6100	57.234	57.4899	1.61950	1.6137	1.6083	1.6017	(211)
66.3281	66.97	67.18	1.4023	1.3977	1.3961	1.3923	(202)
70.9431	71.3118	71.3897	1.3213	1.3221	1.3218	1.3202	(221)
75.3203	75.8211	76.123	1.2537	1.2598	1.2566	1.25401	(310)

As shown in Fig. 2, the lattice constant decreased when the temperature increased. Overall, it can be seen that the lattice constant and tetragonality gradually decreased with increasing high temperature. At the high temperature of 1200 °C, the tetragonality was close to 1, showing that $Ba_{0.7}Sr_{0.3}TiO_3$ gradually changed from a tetragonal to a pseudo-cubic phase with increased temperatures.

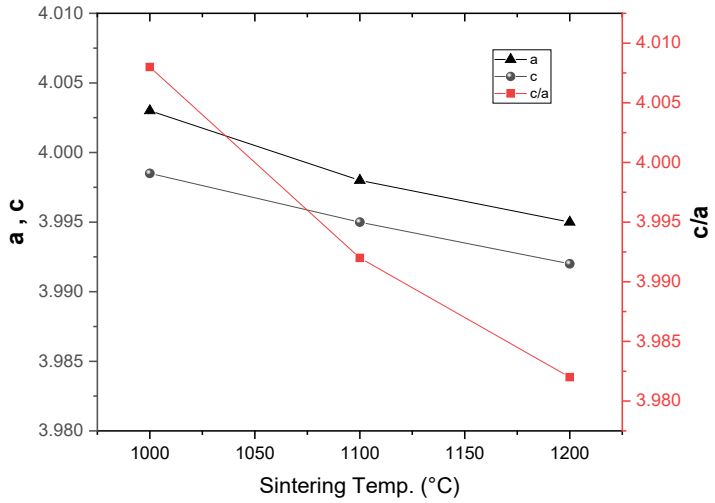

Fig. 2. The relationship between sintering temperature and the lattice constant and tetragonality of Ba0.7Sr0.3TiO3 ceramics.

The sintering of $Ba_{0.7}Sr_{0.3}TiO_3$ the powder at 1000, 1100 and 1200 degrees Celsius showed very grain size with spherical or cubic shape particles, as can be seen from the FESEM images of the samples in Fig. 3. As a result of the FESEM morphological surface, the particle size of powders grew as the temperature increased. According to Fig. 3, the calculated grain size of $Ba_{0.7}Sr_{0.3}TiO_3$ treating at 1000 °C, 1100, and 1200 °C was 112.88, 221.44 nm and 397.39 nm, respectively. The ImageJ program (1.51j8) showed that the particle size increased with increased high temperature.

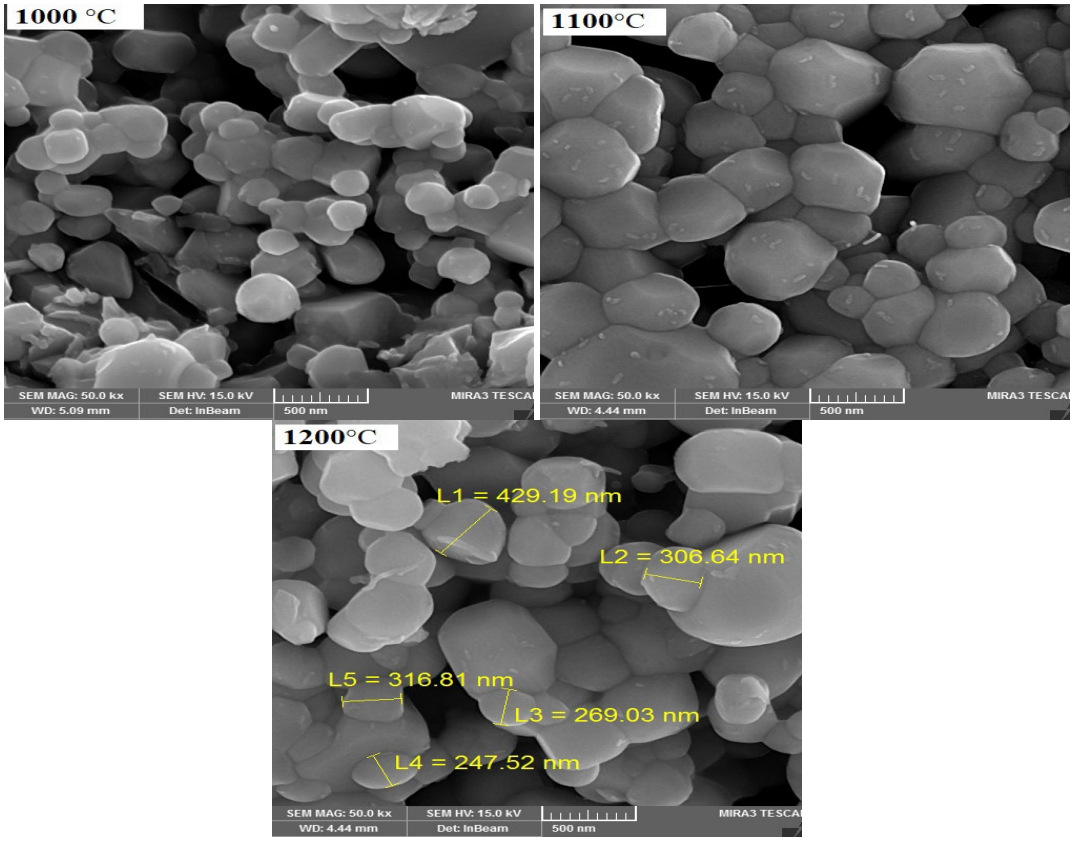

Fig. 3. FESEM micrograph of ferroelectric $Ba_{0.7}Sr_{0.3}TiO_3$ at various temperatures (a) 1000 °C, (b) 1100 °C, and (c) 1200 °C.

Fig. 4 shows how the dielectric characteristics of Ba0.7Sr0.3TiO3 alter depending on different high temperatures. Firstly, it was found that the dielectric constant of $Ba_{0.7}Sr_{0.3}TiO_3$ treated at (1000, 1100 and 1200˚C) decreased as the frequency increased. It attributed to different polarization mechanisms (electronic, atomic or ionic, orientation, dipolar, and space charge polarisation), which affected the total polarization. At low frequencies, all types of polarization were affected by increased frequencies. Some types of polarization could not catch up with the relaxed time of the frequencies, while others disappeared when the frequencies were increased or with high frequency.

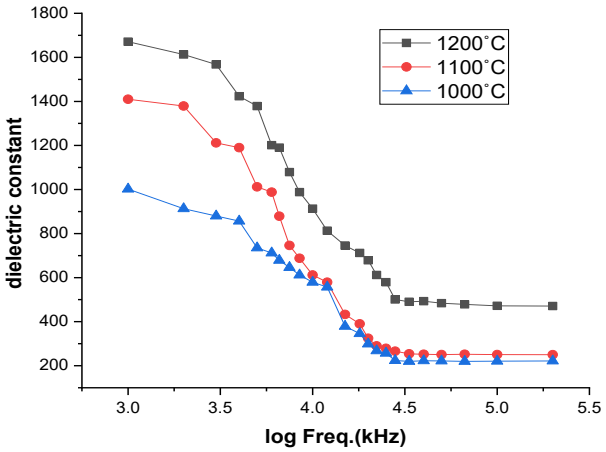

Fig. 4. The dielectric constant vs. frequency at different temperatures.

The same graph concludes that the dielectric constant increased when the sintering temperature rose. The dielectric constant values are equal to (1011, 1422, and 1711) for (1000, 1100, and 1200˚C), respectively. The fluctuation in the values is attributed to the change in particle size with increased high treat temperature. The sample is treated at a high temperature to get the best crystalline structure, fewer vacancies, and high density, so it has a high value of the dielectric constant.

The dissipation factor of $Ba_{0.7}Sr_{0.3}TiO_3$ sintering at (1100 °C and 1200 °C) decreased with increasing temperature, as shown in Fig.5. The dissipation factor of the sample at (1000 °C) was greater than the sample at (1100 °C), which is the stabilized sample, when the sintering temperature was increased, due to reduced porosity and higher density.

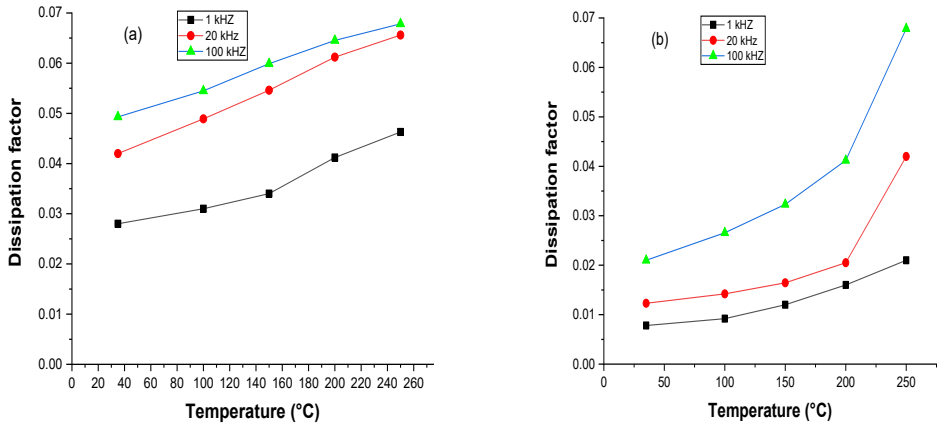

Fig. 5. Dissipation factor for Ba0.7Sr0.3TiO3 for (1000 & 1100˚C).

The physical properties and fabrication process of the $Ba_{0.7}Sr_{0.3}TiO_3$ compound greatly affect the value of its dielectric constant and dissipation factor. The high treatment temperature affects the degree of crystallization, which, in turn, affects the values of the dielectric constant and dissipation factor. Compared to its dielectric constant, the porosity, crystallinity, and particle size of the BST compound were significantly more affected by the changing temperatures (1100 °C, 1200 °C).

Fig. 6 also illustrates the dielectric properties as a function of temperature and different frequencies (1 kHz, 20 kHz, and 100 kHz).

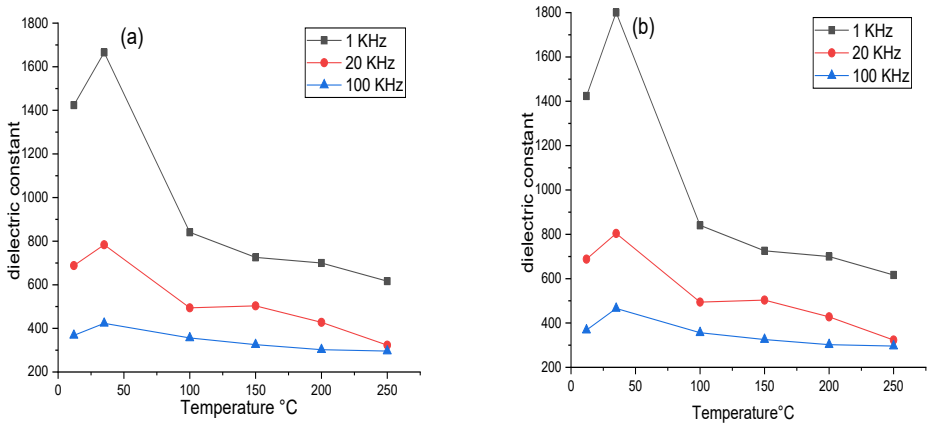

Fig. 6. The dielectric constant vs temperatures with different frequencies (1,20,100 kHz).

The dielectric constant initially increased when the temperature was increased to the critical temperature, i.e. the Curie temperature, where the maximum dielectric constant was achieved. Then, the dielectric constant decreased with increased temperature and increased dissipation factor. $Ba_{0.7}Sr_{0.3}TiO_3$ is a tetragonal structure within the Curie temperature range of (28–30) °C. Above the transition temperature, the dielectric constant goes down because the molecules' thermal oscillations and the dipoles' degree of disorder increase.

4. Conclusion

Using the sol-gel method, the raw materials used to prepare the $Ba_{0.7}Sr_{0.3}TiO_3$ compound were barium acetate, strontium acetate, and titanate (IV) isopropoxide. The solvent used acetic acid to solve Ba and Sr acetate and the stabilizer for the Ti(IV) structure using 2-methoxy ethanol. The effect of different sintering temperatures on the particle size, dielectric constant, and dissipation factor is obtained. The XRD pattern showed a tetragonal perovskite structure for the $Ba_{0.7}Sr_{0.3}TiO_3$ compound with a lattice constant (a = b =3.9771 Å) and P4 mm space group (221). The d-spacing decreased when the sintering temperature was increased because of a change in particle size. FESEM was used to determine the size of the particles. The results showed that the particle sizes varied (112.88, 221.44 nm and 397.39 nm, respectively) with varying sintering temperatures. Also, the particle size increased with increased sintering temperature. Increasing the sintering temperature led to an increased dielectric constant that attributed to an increase in particle size, density and decreased lattice constant. The dielectric constant decreased when increasing the frequency and temperature.

Acknowledgements

The authors would like to express their gratitude to everyone who assisted them in the completeion of this study.

References

[1] H. A. Gatea, I. S. Naji, and A. F. Abulameer, Int. J. Thin Film Sci. Technol., vol. 9(2), 2020, doi: 10.18576/ijtfst/090208; https://doi.org/10.18576/ijtfst/090208

[2] H. A. Gatea and I. S. Naji, J. Adv. Dielectr., vol. 10(5), 2020; https://doi.org/10.1142/S2010135X20500216

[3] O. A. Alawi et al., Sustain. Energy Technol. Assessments, vol. 49, 2022; https://doi.org/10.1016/j.seta.2021.101772

[4] H. A. Gatea, J. Mater. Sci. Mater. Electron., vol. 34(6), 2023; https://doi.org/10.1007/s10854-023-09860-3

[5] Z. M. Y. li Omran Al-Sulttani, Mohammed Suleman Aldlemy, Musaddak M Abdul Zahra, Hamed A Gatea, Khaled Mohamed Khedher, Miklas Scholz, Energy Reports, vol. 8, pp. 1867-1882; https://doi.org/10.1016/j.egyr.2022.01.007

[6] H. A. Gatea and S. M. Khalil, Eur. Phys. J. D, vol. 76, no. 8, 2022; https://doi.org/10.1140/epjd/s10053-022-00462-y

[7] S. P. P. Sadhu et al., Appl. Phys. B Lasers Opt., vol. 124, no. 10, p. 0, 2018; https://doi.org/10.1007/s00340-018-7062-2

[8] G. Liu and C. W. Nan, J. Phys. D. Appl. Phys., vol. 38, no. 4, pp. 584-589, 2005; https://doi.org/10.1088/0022-3727/38/4/010

[9] A. Ioachim et al., Prog. Solid State Chem., vol. 35, no. 2-4 SPEC. ISS., pp. 513-520, 2007; https://doi.org/10.1016/j.progsolidstchem.2007.01.017

[10] R. M. Piticescu, P. Vilarnho, L. M. Popescu, and R. R. Piticescu, J. Optoelectron. Adv. Mat.

8(2), 543 (2006).
[11] Y. Xu, Ferroelectr. Mater. their Appl., pp. 163-215, 1991; https://doi.org/10.1016/B978-0-444-88354-4.50009-7
[12] E. Yeceu, H. Laysandra, and D. Triyono, J. Phys. Conf. Ser., vol. 1442, no. 1, pp. 1-5, 2020; https://doi.org/10.1088/1742-6596/1442/1/012020
[13] B. Nagaraj et al.,Appl. Phys. Lett., vol. 74, no. 21, pp. 3194-3196, 1999; https://doi.org/10.1063/1.124104
[14] J. Zhang, Phd Thesis, 2013.
[15] H. A. Gatea, Int. J. Thin Film Sci. Technol., vol. 10(2), pp. 95-100, 2021; https://doi.org/10.18576/ijtfst/100204
[16] V. A. Vasiljev, K. A. Vorotilov, M. I. Yanovskaya, L. I. Solovjeva, and A. S. Sigov, J. Sol-Gel Sci. Technol., vol. 13(1-3), pp. 877-883, 1998; https://doi.org/10.1023/A:1008615021712
[17] H. A. Gatea, Nanosci. Nanotechnology-Asia, vol. 11(3), pp. 322-329, 2020; https://doi.org/10.2174/2210681210999200715105250
[18] A. A. Ansari, P. R. Solanki, and B. D. Malhotra, Appl. Phys. Lett., vol. 92(26), pp. 2006-2009, 2008; https://doi.org/10.1063/1.2953686
[19] A. Selmi, O. Khaldi, M. Mascot, F. Jomni, and J. C. Carru, J. Mater. Sci. Mater. Electron., vol. 27(11), pp. 11299-11307, 2016; https://doi.org/10.1007/s10854-016-5253-3
[20] J. Wang, X. Yao, and L. Zhang, Ceram. Int., vol. 30(7), pp. 1749-1752, 2004; https://doi.org/10.1016/j.ceramint.2003.12.134
[21] W. Rao, D. Li, and H. Yan, Adv. Mater. Res., vol. 621, pp. 23-26, 2013; https://doi.org/10.4028/www.scientific.net/AMR.621.23
[22] M. Guglielmi, G. Kickelbick, and A. Martucc, (Advances in Sol-Gel Derived Materials and Technologies). 2014.
[23] D. Shiferaw, S. Kasam, S. Kena, and K. Legesse, Sci. Technol. Arts Res. J., vol. 3, no. 4, p. 89, 2015; https://doi.org/10.4314/star.v3i4.13